Eur. Phys. J. A (2016) **52**: 86
DOI 10.1140/epja/i2016-16086-1

THE EUROPEAN PHYSICAL JOURNAL A

Review

α/β discrimination in Borexino*

C. Galbiati[1,a], M. Misiaszek[2,3], and N. Rossi[3]

[1] Physics Department, Princeton University, Princeton, NJ 08544, USA
[2] M. Smoluchowski Institute of Physics, Jagiellonian University, 30059 Krakow, Poland
[3] INFN Laboratori Nazionali del Gran Sasso, SS 17 bis Km 18+910, 67010 Assergi (AQ), Italy

Received: 13 July 2015
Published online: 18 April 2016 –
Communicated by C. Broggini

Abstract. In this report we describe the unique capabilities of the α/β discrimination of the Borexino experiment. This capability is the direct result of years of development aimed at the design of an experiment that could withstand contamination from α-emitting nuclides. The combination of the excellent α/β discrimination and of the excellent radiopurity of the detector permitted to extract information on the solar neutrino interactions in Borexino without interference from α particles.

The Borexino solar neutrino experiment [1] was designed to detect solar neutrinos by means of their elastic scattering on electrons in the scintillator. Electron neutrinos (ν_e) interact through charged and neutral currents and in the energy range of interest have a cross section ~ 5 times larger than ν_μ and ν_τ, which interact only via the neutral current. The electrons scattered by neutrinos are detected by means of the scintillation light retaining the information on the energy, while information on the direction of the scattered electrons is lost. The primary object of the investigation of Borexino is the ^{7}Be solar neutrinos, whose basic signature for the mono-energetic 0.862 MeV is the Compton-like edge of the recoil electrons at 665 keV. Borexino has successfully produced the most accurate measurement of ^{7}Be neutrinos [2–4]. Borexino has also produced the first measurement of ^{8}B neutrinos in liquid scintillator with 3 MeV energy threshold [5], the first measurement of *pep* neutrinos [6], and the first real-time measurement of *pp* neutrinos [7].

The key features of the Borexino detector are described in refs. [1, 8]. Borexino is a scintillator detector with an active mass of 278 tons of pseudocumene (PC, 1,2,4-trimethylbenzene), doped with 1.5 g/liter of PPO (2,5-diphenyloxazole, a fluorescent dye). The scintillator is contained in a thin (125 μm) nylon vessel [9, 10] and is surrounded by two concentric PC buffers (323 and 567 tons) doped with 5.0 g/l of dimethylphthalate (DMP), a component quenching the PC scintillation light. The two PC buffers are separated by a second thin nylon membrane to prevent diffusion of radon towards the scintillator. The scintillator and buffers are contained in a Stainless-Steel Sphere (SSS) with diameter 13.7 m. The SSS is enclosed in a 18.0 m diameter, 16.9 m high domed Water Tank (WT), containing 2100 tons of ultrapure water as an additional shield. The scintillation light is detected via 2212 8" PMTs uniformly distributed on the inner surface of the SSS [11–13]. Additional 208 8" PMTs instrument the WT and detect the Cherenkov light radiated by muons in the water shield, serving as a muon veto.

The key requirement in the technology of Borexino is achieving extremely low radioactive contamination, at or below the expected interaction rate of 0.5 counts/(day · ton) expected for ^{7}Be neutrinos. The design of Borexino is based on the principle of graded shielding, with the inner core scintillator at the center of a set of concentric shells of increasing radiopurity. All components were screened and selected for low radioactivity [14], and the scintillator and the buffers were purified on site at the time of filling [15–17]. Position reconstruction of the events, as obtained from the PMTs timing data via a time-of-flight algorithm, allows to fiducialize the active target: approximately 2/3 of the scintillator serves as an active shield.

The foundation of the α/β discrimination in Borexino is in the difference of the time profile (pulse shape) of the organic liquid scintillator which is the target of the detector. The parameters of the pulse shape, along with the measurements of the long R&D campaign that led to the selection of the scintillator for the Borexino target, are well detailed in ref. [18].

For each event, the time of arrival of the first photoelectron on each PMT is recorded. As described in ref. [2], for each detected photon the arrival time and the charge

* Contribution to the Topical Issue "Underground nuclear astrophysics and solar neutrinos: Impact on astrophysics, solar and neutrino physics" edited by Gianpaolo Bellini, Carlo Broggini, Alessandra Guglielmetti.

[a] e-mail: galbiati@princeton.edu

are measured by means of a suitable analog and digital electronics chain. The Borexino main trigger fires when at least 30 PMTs each detect at least one photoelectron within a time window of 100 ns, corresponding to an energy threshold of approximately 60 keV. When a trigger occurs, the time and the charge of each PMT that has detected at least one photoelectron in a time gate of 7.2 μs is recorded. The time is measured by a Time-to-Digital Converter (TDC) with a resolution of about 0.5 ns, while the charge (after integration and pulse shaping) is measured by means of an 8 bit Analog-to-Digital Converter (ADC). This time resolution is smaller than the intrinsic time jitter of the PMTs which is 1.1 ns.

Offline analysis codes were employed to reconstruct the time, charge and position of each recorded event. As a first step in the offline analysis, the codes identify in the recorded gate the clusters, that is, groups of time-correlated hits that belong to a unique physical event. Generally, only one cluster is found in each event gate, but in the case of fast coincidences like ^{212}Bi-^{212}Po and ^{85}Kr-^{85m}Rb, or in the case of accidental pile up, more than one scintillation event may be recorded within the same trigger gate, yielding more than one reconstructed cluster from one event. Piled-up events resulting from the superposition of two different scintillation events within a few hundred ns are identified and rejected in the course of the analysis. The position is then determined using a photon time-of-flight likelihood method based on probability density function (pdf) derived from Monte Carlo simulations and checked on the CTF and in Borexino [19]. The resolution in the event position reconstruction is approximately 13 ± 2 cm in each of the three coordinates at the relatively high ^{214}Bi-^{214}Po energies. The spatial resolution is expected to scale as $\sqrt{N}$, where N is the number of detected photoelectrons [20].

The basic selection criteria of event in Borexino are performed by means of the following cuts:

i) Events must have a unique time cluster of PMTs hits, to reject pile-up of multiple events in the same acquisition window.
ii) Muons and all events within a time window of 2 ms after a muon are rejected.
iii) Decays due to radon daughters occurring before the ^{214}Bi-^{214}Po delayed coincidences are vetoed. The fraction surviving the veto is accounted for in the analysis.
iv) Events must be reconstructed within a spherical fiducial volume corresponding approximately to 1/3 of the scintillator volume in order to reject external γ background. Additionally, we require the z-coordinate of the reconstructed vertex, measured from the center of the detector in the vertical direction, to satisfy $|z| < 1.7$ m in order to remove background near the poles of the inner nylon vessel.

The combined loss of fiducial exposure due to the cuts i)–iii) is negligible (less than 1%). The fiducial cut iv results in a fiducial mass of approximately 80 tonne.

After the application of the cuts described above, the ^{210}Po α peak, that falls almost completely within the ^{7}Be energy window, lies 2–3 orders of magnitude above the rest of the spectrum. The peak tails, if not properly modelled in the fit procedure, might bias the final results of the ^{7}Be neutrino interaction rate. α particles and β-like (recoil electron or beta decay) events can be identified with limited accuracy, *e.g.* by means of the mean time of the hits in the cluster and of the ratio between the number of hits in the tail and the total number of hits (tail-to-total ratio). In addition, a more efficient identification of α/β can be performed by using discriminating procedures like the Gatti optimal filter [18].

In particular, the latter allows us to separate two classes of events with different but known time distributions of the detected light. For these two classes of events normalized reference shapes $P_1(t)$ and $P_2(t)$ are created by averaging the time distributions of large sample of events. These events are selected without any use of pulse shape variables from the ^{214}Bi-^{214}Po coincidences used as clean samples of α and β events. The functions $P_1(t)$ and $P_2(t)$ represent the probability that a photoelectron is detected at the time between t and $(t + \mathrm{d}t)$ for events of the two classes. The reference shape is binned into $r_1(t_n)$ and $r_2(t_n)$

$$r_{1,2}(t_n) = \int_{t_0+n\Delta t}^{t_0+(n+1)\Delta t} P_{1,2}(t)\mathrm{d}t, \tag{1}$$

where n is the bin number, t_0 is a reference point of the time distribution, and Δt is the bin width.

Let $e(t_n)$ be the measured binned time distribution of the light for each event. The Gatti parameter G is defined as

$$G = \sum_n e(t_n)w(t_n), \tag{2}$$

where $w(t_n)$ are weights given by

$$w(t_n) = \frac{r_1(t_n) - r_2(t_n)}{r_1(t_n) + r_2(t_n)}. \tag{3}$$

The G parameter follows a probability distribution with the mean value $\overline{G}_i$ that depends on particle type:

$$\overline{G}_i = \sum_n r_i(t_n)w(t_n). \tag{4}$$

The corresponding variance σ_G

$$\sigma_{G_i} = \frac{1}{N}\sum_n r_i(t_n)w^2(t_n) - \overline{G_i} \tag{5}$$

is expected to be energy dependent. In the scintillator used by Borexino α pulses are slower and have therefore a longer tail with respect to β pulses. The reference shapes $r_\alpha(t_n)$ and $r_\beta(t_n)$ are shown in fig. 1, while the distributions of the corresponding G parameters (G_α and G_β) are shown in fig. 2. The two distribution are not fully separated as the left tail of G_α extends to negative values and the right tail of G_β extends to positive values. We can conclude that when the number of α events largely exceeds that of the β's, an event-by-event cut throwing away α's with high efficiency while keeping all of the β's is not possible if only based on the $G_{\alpha\beta}$ value. In order to solve this

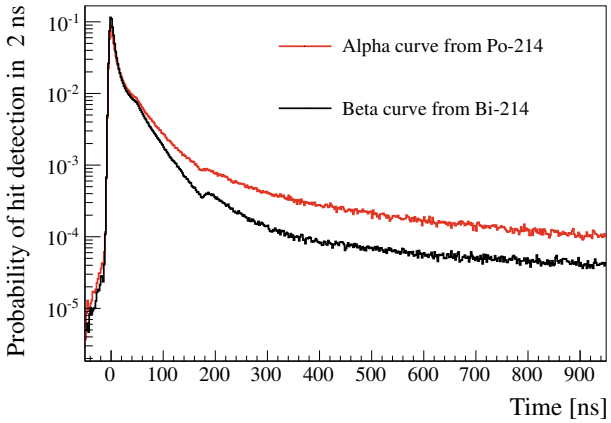

Fig. 1. The reference $r_\alpha(t_n)$ (red) and $r_\beta(t_n)$ (black) pulse shapes obtained by tagging the radon-correlated ^{214}Bi-^{214}Po coincidences. The dip at 180 ns is due to the dead time on every individual electronic channel applied after each detected hit. The small shoulder around 60 ns is due to the reflected light on the SSS surface and on the PMTs cathodes.

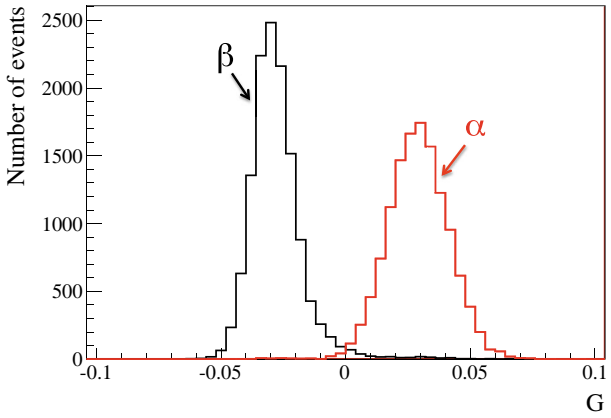

Fig. 2. The distribution of G_α (red) and G_β (black) (see eq. (2)) for events obtained by tagging the radon-correlated ^{214}Bi-^{214}Po coincidences.

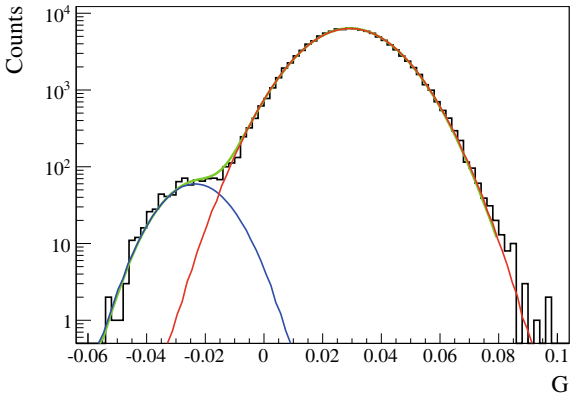

Fig. 3. Example of α-β statistical subtraction with the analytical curves for events in the energy range $200 < N_{pe}^d < 205$. The blue and red lines show the individual Gaussian fits to the Gatti parameter distributions for the β and α components, respectively, while the green line is the total fit.

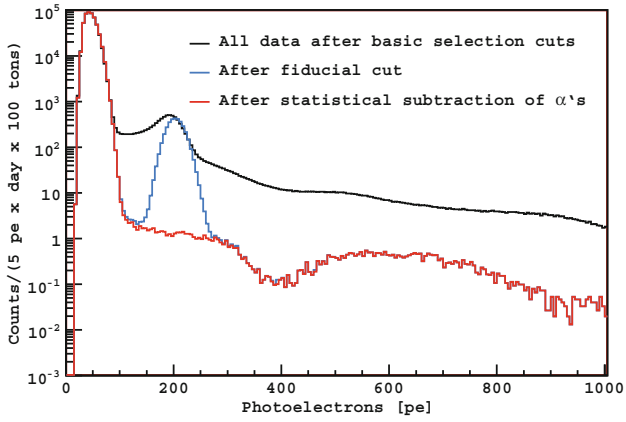

Fig. 4. The raw photoelectron charge spectrum after the basic cuts i)–iii) (black), after the fiducial cut iv) (blue), and after the statistical subtraction of the α-emitting contaminants (red). All curves scaled to the exposure of 100 day·ton. Cuts described in the text.

problem an algorithm for a statistical separation of the α- and β-induced signals was developed. As (5) is energy dependent, for each bin in the energy spectrum, the $G_{\alpha\beta}$ distribution of the data is fitted to two analytical curves which model the distribution of the G_α and G_β. The integral of the fitted curves represents the relative population of each species in the energy bin.

The G_α and G_β distributions are assumed to be Gaussian. The fit procedure also provide the error of the estimated particle population. In bins where one species greatly outnumbers the other, for example in the energy region of the ^{210}Po peak, the means of the Gaussians are fixed to their predicted values.

Figure 3 shows an example of the $G_{\alpha\beta}$ parameter of the data in the energy range $200 < N_{pe}^d < 205$ and its fit with the analytical model. In such a situation the double Gaussian fit, known to be biased, is corrected according to the simulation corresponding to the same population ratio.

The statistical subtraction can be applied in the full ^{7}Be energy window, removing α background coming from isotopes such as ^{210}Po, ^{222}Rn, and ^{218}Po. The error associated to the statistical subtraction is propagated as systematics on the final neutrino interaction rates.

The Borexino spectrum presented in fig. 4 shows the effect on the main analysis cuts. The black curve is the spectrum of all events surviving the basic cuts i)–iii): below 100 photoelectrons (pe) the spectrum is dominated by ^{14}C decays (β^-, $Q = 156$ keV) intrinsic to the scintillator [21] and the peak at 200 pe is due to ^{210}Po decays (α, $Q = 5.41$ MeV, light yield quenched by ~ 13), a daughter of ^{222}Rn out of equilibrium with the other isotopes in the sequence. The blue curve is the spectrum after the fiducial cut iv). The red curve is the final spectrum after the statistical subtraction of the α-emitting contaminants. Prominent features after removing ^{210}Po peak and other minor α backgrounds include the Compton-like edge due to ^{7}Be solar neutrinos (300–350 pe) and the spectrum of

^{11}C (β^+, $Q = 1.98\,\mathrm{MeV}$, created *in situ* by cosmic-ray–induced showers, 400–800 pe). The procedure of using the pulse shape discrimination in PC-based scintillator [18] allow us to extract from the spectral fit the main neutrino fluxes present in the residual β-like spectrum.

Thanks to its satisfying discrimination power, the Gatti filter has been applied in many Borexino analyses also as *soft cut* for pre-selecting events and *hard cut* to locate the main α contaminants as the ^{210}Po within the fiducial volume and for understanding the nature of the main backgrounds [22], *e.g.* in the geo-neutrino analysis [23]. The tuning of the $G_{\alpha\beta}$ parameter played a crucial role in understanding the complexity of the event reconstruction and the most important Borexino results rely on its impressive features.

References

1. Borexino Collaboration (G. Alimonti *et al.*), Astropart. Phys. **16**, 205 (2002).
2. Borexino Collaboration (C. Arpesella *et al.*), Phys. Lett. B **658**, 101 (2008).
3. Borexino Collaboration (C. Arpesella *et al.*), Phys. Rev. Lett. **101**, 091302 (2008).
4. Borexino Collaboration (G. Bellini *et al.*), Phys. Rev. Lett. **107**, 141302 (2011).
5. Borexino Collaboration (G. Bellini *et al.*), Phys. Rev. D **82**, 033006 (2010).
6. Borexino Collaboration (G. Bellini *et al.*), Phys. Rev. Lett. **108**, 051302 (2012).
7. Borexino Collaboration (G. Bellini *et al.*), Nature **512**, 383 (2014).
8. Borexino Collaboration (G. Alimonti *et al.*), Nucl. Instrum. Methods A **600**, 568 (2009).
9. J. Benziger *et al.*, Nucl. Instrum. Methods A **582**, 509 (2007).
10. L. Cadonati, F. Calaprice, C. Galbiati, A. Pocar, T. Shutt, Int. J. Mod. Phys. A **29**, 1442004 (2014).
11. A. Ianni, P. Lombardi, G. Ranucci, O.Ju. Smirnov, Nucl. Instrum. Methods A **537**, 683 (2005).
12. A. Brigatti, A. Ianni, P. Lombardi, G. Ranucci, O.Ju. Smirnov, Nucl. Instrum. Methods A **537**, 521 (2005) 10.1016/j.nima.2004.07.248.
13. L. Oberauer, C. Grieb, F. von Feilitzsch, I. Manno, Nucl. Instrum. Methods A **530**, 453 (2004).
14. Borexino Collaboration (C. Arpesella *et al.*), Astropart. Phys. **18**, 1 (2002).
15. J. Benziger *et al.*, Nucl. Instrum. Methods A **587**, 277 (2008).
16. J. Benziger *et al.*, Nucl. Instrum. Methods A **608**, 464 (2009).
17. H. Simgen, G. Zuzel, *Ultrapure gases - From the Production Plant to the Laboratory*, in *AIP Conference Proceedings*, Vol. **897**, *Topical Workshop on Low Radioactivity Techniques: LRT 2006, Aussois (France)*, edited by P. Loaiza (Springer, 2007) pp. 45–50.
18. Borexino Collaboration (H.O. Back *et al.*), Nucl. Instrum. Methods A **584**, 98 (2008).
19. Borexino Collaboration (G. Alimonti *et al.*), Astropart. Phys. **8**, 141 (1998).
20. C. Galbiati, K. McCarty, Nucl. Instrum. Methods A **568**, 700 (2006).
21. Borexino Collaboration (G. Alimonti *et al.*), Phys. Lett. B **422**, 349 (1998).
22. Borexino Collaboration (G. Bellini *et al.*), Phys. Rev. D **89**, 112007 (2014).
23. Borexino Collaboration (G. Bellini *et al.*), Phys. Lett. B **722**, 295 (2013) arXiv:1303.2571 [hep-ex].